

Response of RF Networks to Transient Waveforms: Interference in Frequency-Hopped Communications

Gregory J. Mazzaro, *Student Member, IEEE*, Michael B. Steer, *Fellow, IEEE*,
Kevin G. Gard, *Member, IEEE*, and Aaron L. Walker, *Member, IEEE*

Abstract—The long-tail transient responses of a bandpass network to pulsed and switched-tone stimuli are examined and a time-domain closed-form expression of the envelope response is developed. It is shown that the long-tail response leads to interference in frequency-hopping communication systems. Interference, and in particular co-site interference, can result in any radar, communication, or RF sensor system becoming exposed to unintentional pulsed RF signals. In the experimental study, 900-MHz Chebyshev bandpass filters are considered.

Index Terms—Bandpass filters, communication system performance, filter distortion, frequency hop communication, time-frequency analysis, transient response.

I. INTRODUCTION

ANALYSIS OF systems in both the time and frequency domains provides insight into co-site interference, a problem that has long affected communication systems. Co-site interference occurs when multiple radios in close proximity inadvertently operate within the same frequency channel at the same time or otherwise produce spurious tones that degrade the received signal-to-noise ratio. It is known to be caused by circuit-field coupling between nearby radios, and by spectral content produced by nonlinear mixing within nearby radios.

Traditional RF and microwave design has used steady-state analysis in mitigating interference sources such as these. Recent work has uncovered additional sources of co-site interference, such as passive intermodulation distortion (PIM) produced by electrothermal interactions [1]. In this case PIM derives from a long-tail effect that results from the interaction of electrical and thermal systems. In this paper it is shown that long-tail effects occur even in lumped-element circuits, e.g., filters, when excited by pulsed RF signals. Systems with long-tail effects must be analyzed in the time domain although their effect on intermodulation distortion is manifested using a necessarily time-limited frequency-domain description. This paper focuses on communication systems that use bursty transmissions because many radios operating in ad-hoc environments use frequency-hopping

techniques that are susceptible to co-site interference due to transients that last longer than expected.

An understanding of the bandpass nature of radio-frequency networks provides insight into the causes and effects of long-tail waveforms. This paper summarizes the prior analysis of transient distortion in bandpass systems and shows that transient effects are measurable in cellular-band communication systems. The cause of long-tail transients is related to the structure of a bandpass filter, and switched-tone output waveforms are explained as an interference phenomenon. It is shown that low-pass prototyping reduces the complexity of full differential equation solutions, and transient effects are evaluated on a typical frequency-hopping communication scenario.

II. BACKGROUND

The study of transient effects in narrowband systems can be traced back to the introduction of FM radio. Carson and Fry noted the existence of a transient term in their mathematical treatment of frequency modulation distortion [2]. The transient behavior of multipole filters was not studied in detail until Tucker and Eaglesfield developed time-domain expressions for amplitude overshoot and settling time for commonly used six-element filters excited by single-tone pulses [3]–[6].

Hatton analyzed the response of a parallel RLC circuit to a single discrete frequency step (switched-tone pulse) and observed considerable amplitude overshoot for frequencies within a circuit's passband [7]. McCoy noticed that transient envelopes were strongly dependent upon the order in which tones were applied and demonstrated that transients became longer as the number of coupled filtering stages increased [8]. Salinger showed that transients also became longer as circuit bandwidth was reduced [9].

Weiner and Leon computed bounds on amplitude overshoot as a function of filter bandwidth and frequency step for coupled single-tuned circuits and Butterworth filters up to third order, and they provided traces of measured frequency transients for a single-tuned circuit with different combinations of input frequencies [10]. Hartley developed a closed-form solution for instantaneous amplitude, phase, and frequency of the transients, and generated plots for single- and double-tuned filters [11]. Chohan and Fidler generalized Hartley's results for second-order Butterworth filters [12].

Studies of transient distortion have not been extended to bandpass filters above third order, and no data have been presented to evaluate the effects of such distortion on frequency-hopped communications for filters of any design.

Manuscript received June 12, 2008; revised September 13, 2008. First published November 07, 2008; current version published December 05, 2008. This work was supported by the U.S. Army Research Office under Grant W911NF-07-1-0004 and by a Multidisciplinary University Research Initiative under Grant W911NF-05-1-0337.

G. J. Mazzaro, M. B. Steer, and K. G. Gard are with the Department of Electrical and Computer Engineering, North Carolina State University, Raleigh, NC 27695-7914 USA (e-mail: gjmazzar@ncsu.edu).

A. L. Walker is with Vadum Inc., Raleigh, NC 27606 USA (e-mail: aaron.walker@vaduminc.com).

Color versions of one or more of the figures in this paper are available online at <http://ieeexplore.ieee.org>.

Digital Object Identifier 10.1109/TMTT.2008.2007085

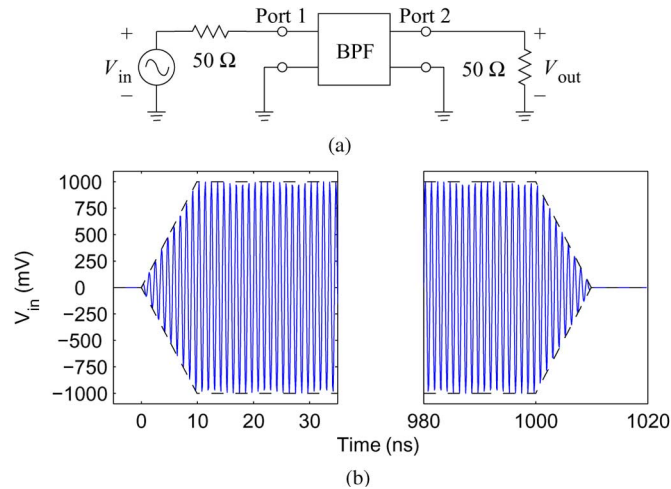


Fig. 1. Transient response test circuit. (a) Schematic. (b) Single-tone stimulus pulse. The synthesizer is an Agilent E8267C vector signal generator which provides pulse rise and fall times of approximately 10 ns.

III. PULSED RESPONSE

Filters used in communications systems are typically of the Chebyshev type as these provide high band selectivity. In this section, a 900-MHz bandpass filter as used in cellular communications is considered. The impact of ringing (or long-tail response) is examined experimentally and in simulation.

A. Experiment

A seventh-order 900-MHz Chebyshev bandpass filter (BPF) with 34-MHz bandwidth was characterized using the circuit of Fig. 1. The schematic is given in Fig. 1(a). The filter was excited by 1- μ s-long single-tone pulses generated by a 100-MS/s digital synthesizer operating near 900 MHz. An example pulse is given in Fig. 1(b). Plots of the filter's transmission response as recorded by a real-time digitizing oscilloscope are shown in Fig. 2 along with a transient simulation of the same envelope response in Agilent's Advanced Design System (ADS) 2006 for a lumped-element filter realization.

The Q of the filter can be related to the inverse of the fractional bandwidth γ so that

$$Q \approx \frac{1}{\gamma} = \frac{f_0}{(f_2 - f_1)} = \frac{900 \text{ MHz}}{34 \text{ MHz}} = 26.5. \quad (1)$$

The time constant τ is the time required for the envelope of the filter's output to reach 63% of its steady-state value, and for this filter it is calculated to be [13]

$$\tau_c = \frac{Q}{2\pi f_0} = \frac{26.5}{(2\pi)(900 \text{ MHz})} = 4.7 \text{ ns}. \quad (2)$$

The simulated and measured data show that 63% of the steady-state response is reached between 75–125 ns. The apparent measured time constant τ_m is much longer than that calculated.

For lower order filters, the approximation given by (1) is valid and (2) accurately estimates the filter settling time. From this example, however, it is clear that for higher order filters, (1) is not valid and (2) does not accurately calculate the settling time.

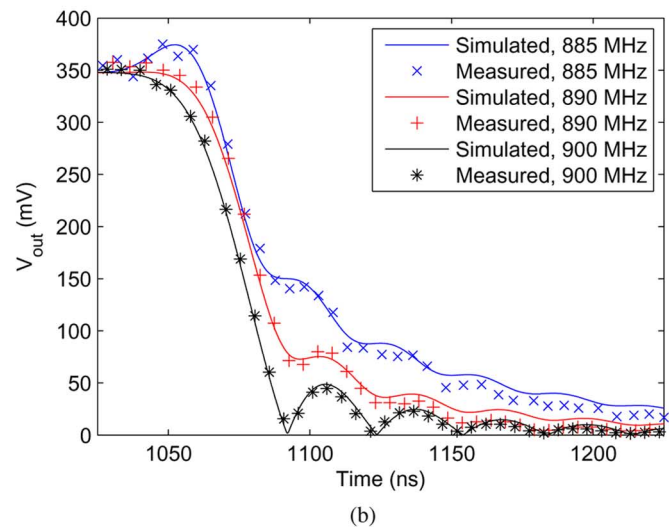
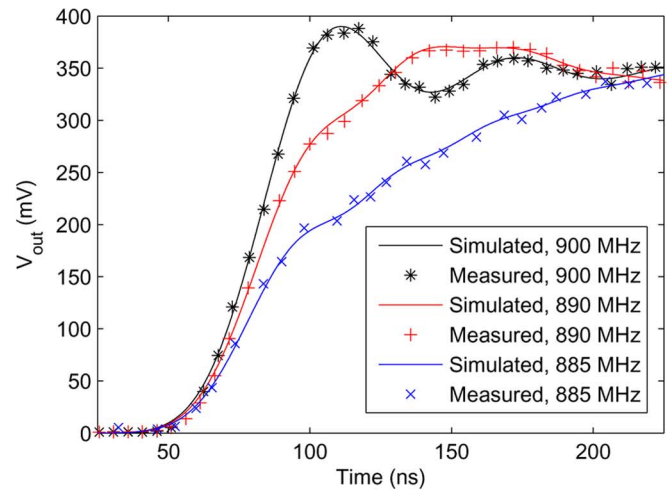


Fig. 2. Step-modulated transmission response envelope as a function of tone frequency. The Chebyshev filter is seventh order with $f_0 = 900$ MHz, BW = 34 MHz (4%), passband ripple = 0.01 dB, insertion loss = 3.15 dB. Stimulus tone switched on at $t = 0$ ns, off at $t = 1000$ ns. (a) Turn-on response. (b) Turn-off response.

B. Discussion

To understand why the measured time constant is longer than expected, $\tau_m \gg \tau_c$, the internal structure of the filter must be examined. While much of the analysis in the literature has been performed on filters containing only one or two resonators, the nature of the long-tail transients requires an understanding of the time-domain interaction of multiple resonators.

Bandpass filters are made up of coupled resonators. Inside each filter, individual sections with similar resonant properties are chained together to form a larger structure whose frequency selectivity meets a particular design criterion. The lumped-element equivalent of a seventh-order bandpass filter is shown in Fig. 3. There are seven resonators in total: four parallel LC tank circuits joined together by three series LC coupling resonators. In order to transmit or reject a signal, a bandpass filter must temporarily store the wave's energy in a resonant structure similar to this one.

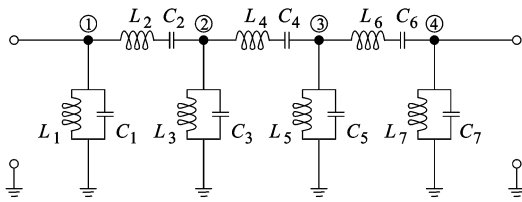


Fig. 3. Lumped-element model of a seventh-order Chebyshev bandpass filter.

TABLE I
TIME REQUIRED TO CHARGE INDIVIDUAL NODES TO 99%
OF STEADY-STATE VOLTAGE VALUE, SIMULATED

Node:	1	2	3	4
900 MHz	7 ns	33 ns	57 ns	77 ns
892 MHz	7 ns	39 ns	83 ns	110 ns
885 MHz	26 ns	423 ns	462 ns	477 ns

Before a signal is applied to the filter, its inductive branches contain no magnetic energy and its capacitive branches contain no electric energy. After a signal is applied, the resonators begin to charge to their steady-state voltages and currents. Energy is stored in the first resonator with a voltage drop across the first capacitor and a current flow through the first inductor. Series coupling allows this energy to cascade through each of the resonant pairs to eventually reach the filter output. The time required to charge each node is dependent not only on the equivalent resistance seen at the node, but on the charging times of all previous nodes in the cascade.

If the frequency of the applied signal is within the filter's passband, wave energy enters the filter, the resonators oscillate in-phase, and most of the wave passes through to the filter output. If the frequency is outside the passband, the resonators oscillate out-of-phase and very little energy appears at the output. If the frequency is well outside the passband, most of the energy does not enter the filter at all; instead it is immediately reflected by the first resonator in the filter chain.

The cascade of wave energy through the simulated filter circuit is illustrated by Table I. Displayed are the times required for each of the nodes in Fig. 3 to charge to 99% of their steady-state voltage values for three different input frequencies. Since Node 1 immediately follows the 50- Ω source termination of the probe circuit [see Fig. 1(a)], the resonant pair L_1C_1 charges to steady-state the fastest. The other resonant pairs follow in cascade. Because the signal must charge each resonator before moving to the next, the output port requires the greatest amount of time to charge.

IV. SWITCHED-TONE RESPONSE

A. Experiment

From Fig. 2(a), it is apparent that the time required to charge the output of the filter to steady-state is strongly dependent upon the applied frequency; the rise time generally increases as the applied tone is moved away from midband. From Fig. 2(b), it is apparent that the time required for the filter's output to discharge to zero follows a similar trend; the fall time also increases as the applied tone is moved away from midband. These trends imply that it is possible to produce an interference pattern between

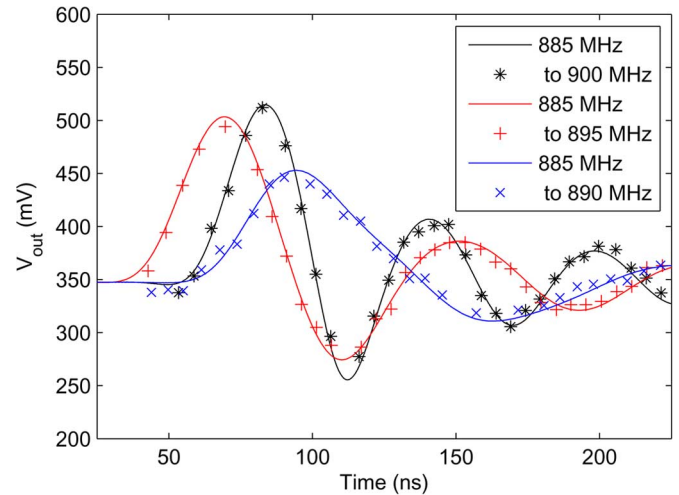


Fig. 4. Switched-tone transmission response envelope as a function of input frequency step size. Seventh-order Chebyshev filter with $f_0 = 900$ MHz, BW = 34 MHz, passband ripple = 0.01 dB, insertion loss = 3.15 dB. Tone switched at $t = 0$ ns.

tones of different frequencies if the input is switched quickly enough between them.

To generate two-tone interference, the digital synthesizer was reprogrammed with a switched-tone probe: a stimulus that switches its frequency between two tones at regular (1 μ s) intervals while maintaining a constant amplitude envelope and a constant phase across the transition. Plots of the switched-tone response of the filter are given in Fig. 4.

B. Discussion

Since the fall time of a pulse response with frequency near to the passband is slow and the rise time of a pulse well within the passband is fast, an interference pattern can be produced by exciting the bandpass filter with a waveform that switches frequency abruptly from a slowly decaying tone to a quickly rising tone. The slowly decaying output at the first frequency overlaps with the quickly charging output at the second frequency, producing two-tone interference for approximately as long as it takes a single tone to decay completely.

This phenomenon can be explained physically by reading Table I up-and-down instead of left-to-right. Since wave energy couples into the resonators more efficiently at frequencies near the center of the filter's passband, the time required for the internal nodes to charge to steady-state generally increases as the applied tone is moved away from midband. This trend implies that pulses of wave energy do not travel through cascaded resonators at equal rates. It is these unequal transit times that cause interference between neighboring pulses.

V. MATHEMATICAL MODELING

A. Prior Approaches

A number of methods for obtaining a closed-form solution for the transient waveforms exist in the relevant literature. While Salinger performed his analysis using complex integration and assuming ideal filters [9], the rest of the approaches are solutions

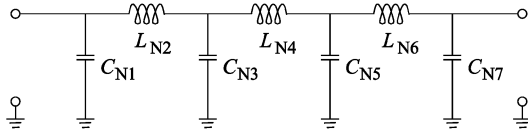


Fig. 5. Low-pass prototype for a seventh-order Chebyshev bandpass filter.

to the differential equations of physically realizable filter circuits. Hatton solved the full differential equation in the time domain for a single resonator [7]. Tucker and Eaglesfield used differential operators, a precursor to Laplace transforms, to obtain solutions to excitations at midband for commonly used third-order filters [3]–[6]. McCoy applied Laplace transforms to generalize the response to any number of resonators, assuming ideal coupling between them [8]. Hartley used assumptions of narrow bandwidth, high Q , and s -domain symmetry to reduce the complexity of the Laplace method [11]. Chohan and Fidler exploited the s -domain shifting property to generalize Hartley’s results to filters of any Q value [12].

Each of the aforementioned methods solves a differential equation of order $2N$, where N is the number of resonators contained in the filter. Also, each of these methods requires that either the bandpass circuit values be specified, or that the bandpass transfer function be given, in order to solve for the time domain output expression. These solutions become increasingly complex for filters of higher order. (For example, the time-domain expression for a seventh-order filter response requires solution of a 14th-order differential equation.) It is possible, however, to greatly simplify the analysis for filters that are designed from low-pass prototypes.

B. Low-Pass Prototyping

Typically, bandpass filter design begins with the filter’s low-pass prototype, a network of series inductances and shunt capacitances, realizing specifications of rolloff, passband ripple, and $1\text{-}\Omega$ resistive terminations. A frequency transformation is then used to center the filter’s passband at the operating frequency and to accommodate a change in resistance at the filter’s input and output ports. The low-pass equivalent of the filter of Fig. 3 is given in Fig. 5.

The same frequency transformation that is used to obtain the bandpass circuit values from their corresponding low-pass equivalent values can be used to obtain the bandpass time-domain response from its low-pass equivalent response. The Laplace domain frequency translation in the narrow-band case is given by [14]

$$s = \frac{\omega_2 - \omega_1}{2} S \pm j\omega_0 \quad (3)$$

where ω_1 and ω_2 are the lower and upper passband frequencies, ω_0 is the center frequency of the filter, s is the bandpass Laplace variable, and S is the low-pass Laplace variable. With respect to their low-pass counterparts, the poles and zeros of the filter are scaled by half of the radian bandwidth of the filter and shifted up to $+j\omega_0$ and down to $-j\omega_0$.

Let the input voltage stimulus and its Laplace transform be

$$V_0 e^{j(\omega_0 + \Delta\omega)t} u(t) \Leftrightarrow \frac{V_0}{s - j(\omega_0 + \Delta\omega)} \quad (4)$$

where $\Delta\omega$ represents the deviation in the excitation frequency from the center of the filter’s passband and V_0 is the amplitude of the applied RF pulse. The low-pass equivalent of this waveform and its inverse Laplace transform are found by shifting and scaling the single pole in the denominator of (4) according to (3)

$$\frac{V_0}{s - j\left(\Delta\omega\left(\frac{2}{\omega_2 - \omega_1}\right)\right)} \Leftrightarrow V_0 e^{j(\Delta\omega(2/\omega_2 - \omega_1))t} u(t). \quad (5)$$

Assuming filter poles with no greater multiplicity than one, the low-pass equivalent response can be written [14]

$$V_{\text{out}}^{\text{lp}}(t) = \sum_{i=1}^n A_i e^{S_i t} + B e^{j(\Delta\omega(2/\omega_2 - \omega_1))t} \quad (6)$$

where A_i and B are the residues at each low-pass pole. The bandpass output is given by

$$V_{\text{out}}^{\text{bp}}(t) = \sum_{k=1}^{2n} A_k e^{s_k t} + \frac{B}{2} e^{j(\Delta\omega + \omega_0)t} + \frac{B}{2} e^{j(\Delta\omega - \omega_0)t} \quad (7)$$

where the transformation of (3) splits each low-pass pole into two bandpass poles with equal residues. Rearranging terms and simplifying gives

$$V_{\text{out}}^{\text{bp}}(t) = \sum_{i=1}^n \frac{A_i}{2} e^{(\omega_2 - \omega_1/2)S_i t} (e^{j\omega_0 t} + e^{-j\omega_0 t}) \quad (8)$$

$$+ \frac{B}{2} e^{j(\Delta\omega)t} (e^{j\omega_0 t} + e^{-j\omega_0 t}) \quad (9)$$

$$= \cos(\omega_0 t) \left[\sum_{i=1}^n A_i e^{S_i (\omega_2 - \omega_1/2)t} + B e^{j\Delta\omega t} \right] \quad (10)$$

$$= \cos(\omega_0 t) V_{\text{out}}^{\text{lp}}\left(\frac{\omega_2 - \omega_1}{2} t\right) \quad (11)$$

which states that the time-domain response of a narrowband bandpass filter to an RF pulse step is equal to a time-scaled version of its low-pass response that modulates a sinusoid at the center frequency of the bandpass filter.

From (6) and (11), the method for determining the bandpass time-domain response can be summarized as follows:

- scale the deviation frequency by $2/(\omega_2 - \omega_1)$;
- find the low-pass response at this new frequency;
- time-scale the low-pass response by $(\omega_2 - \omega_1)/2$;
- multiply the time-scaled response by the filter center frequency.

The filter response to the end of the input pulse is found by determining the circuit’s response to a delayed and inverted version of the input stimulus given by (4) and adding it to the original response. The switched-tone output is found by superimposing two single-tone pulse responses, with the turn-on time of the second pulse equal to the turn-off time of the first pulse. Fig. 6 compares two single-tone time-scaled low-pass prototype

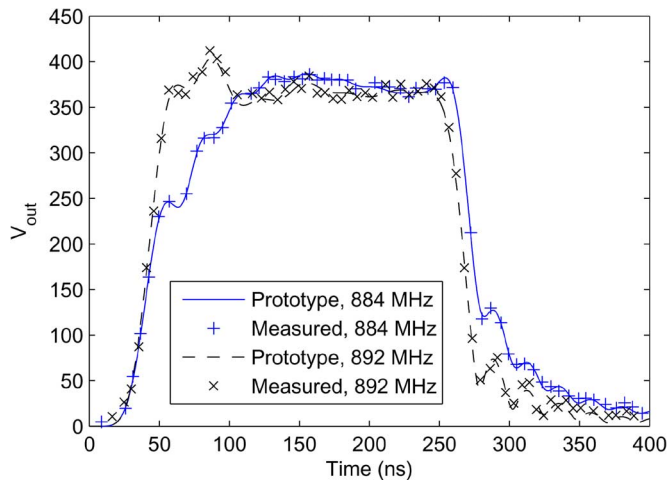


Fig. 6. Time-scaled low-pass prototype envelope versus measured filter output envelope. Seventh-order Chebyshev filter with $f_0 = 900$ MHz, BW = 36 MHz, passband ripple = 0.01 dB, insertion loss = 2.70 dB. Tone switched on at $t = 0$ ns, off at $t = 250$ ns.

envelopes with RF pulse outputs from another cellular-band filter. The RF envelopes show very good agreement.

The time-scaled low-pass prototype method does not require the solution of a $2N$ th order differential equation. Traditional Laplace methods can be used to solve the N th order circuit equation for a filter's low-pass prototype, and the aforementioned frequency- and time-scaling relationships can be used to upconvert the low-pass response to the frequency band of interest. Compared to prior approaches, the complexity of the differential equation solution is cut in half.

VI. EFFECTS ON FREQUENCY-HOPPING SCHEMES

Due to the extended period of time required for a single-tone pulse response to decay, it is clear that a communication scheme that implements fast frequency switching between user pulses has an upper limit to its frequency-switching rate as a result of filtering. Fig. 7 gives the 95% settling time plotted against stimulus frequency for a filter previously analyzed. It is apparent from the simulated data that a communications scheme containing this filter cannot switch frequencies faster than once every 80 ns, even at midband, without causing a significant portion of each pulse to bleed into its neighboring time-slots.

A. Group Delay

The group delay of the simulated filter is also plotted in Fig. 7. As can be seen in this figure, there is very little correlation between the settling time of the pulse responses and the group delay of the filter. The pulse response curve is approximately parabolic both inside and outside of the filter's passband, whereas the group delay displays similar curvature solely within the passband. Outside this region, the group delay is monotonically decreasing beyond its peaks near each passband edge, a phenomenon which is true of all practical multiple bandpass filters [14].

Since group delay is a steady-state quantity, it is generally not relevant for describing transient behavior. If the signal bandwidth (considering a single pulse) is small, corresponding to

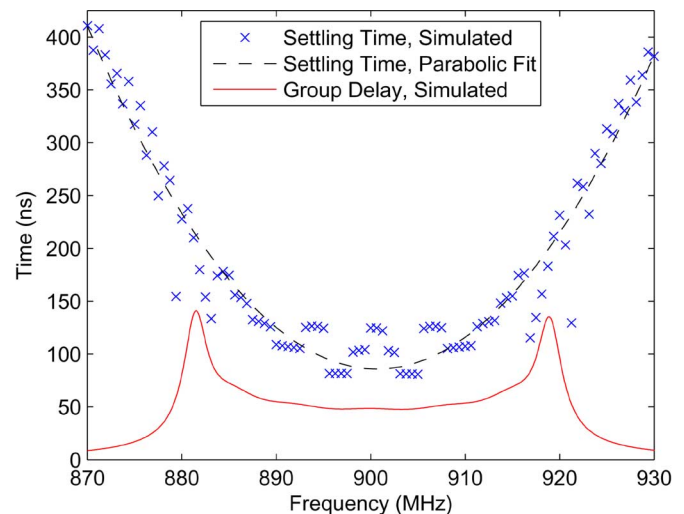


Fig. 7. Time for filter output to settle to 5% of its steady-state value after input has been switched off, compared with group delay. The filter is the same as in Fig. 2.

longer pulse periods and slower rise and fall times, then the group delay characteristic may indeed be used to estimate the time required for a single pulse to traverse the filter. In this case, the system is said to be quasi-stationary: transient effects between pulses are minimal and steady-state analysis is adequate to describe system behavior. A system designer can easily estimate the transmission times for operating frequencies by reading values from the group delay curve. If the signal bandwidth is large, corresponding to short periods and faster transitions, however, the group delay characteristic cannot be used to estimate pulse travel time because the system is not near steady state. To a system designer, it is unclear what the transmission time of a pulse will be when the bandwidth of the pulse is a significant fraction of the filter bandwidth; this information is not readily available from the group delay curve.

B. Example Communication Scenario

An example of the impact that filter transients can have on a multiuser frequency-hopping system is given in Fig. 8. The reception of two data streams that share the same frequency in adjacent time-slots is shown. Fig. 8(a) presents the two filtered user transmissions as separable, but with small overlap near the start of the second pulse. Fig. 8(b) is an expansion of the envelope from Fig. 8(a) near the point of overlap. Fig. 8(b) also shows the result of the superposition of the two pulses.

The superposition shown in Fig. 8(b) is the signal that a frequency-hopping base station would receive. Since the frequency that the first user has just transmitted is the same as the frequency that the second user is currently transmitting, the base station cannot separate the two data streams until the transient response due to the first pulse has become negligible with respect to the second. The extended tail of User 1's transmission appears as interference during User 2's transmission, even if the frequency of operation is well within the filter's passband.

Fig. 9 shows the signal-to-interference ratio (SIR) during reception of the second user's transmission as a function of guard-band length. It is worth noting that the frequency of operation

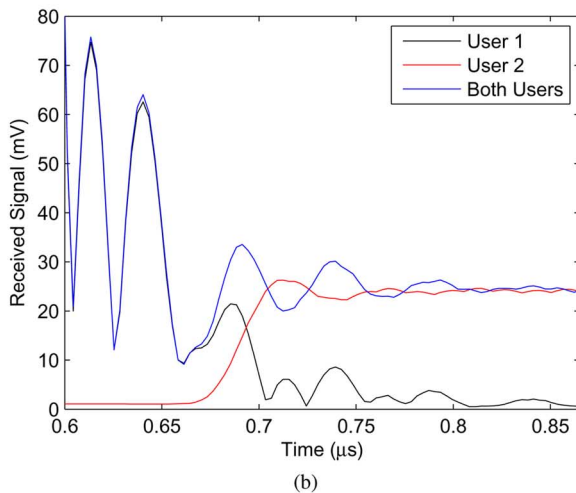
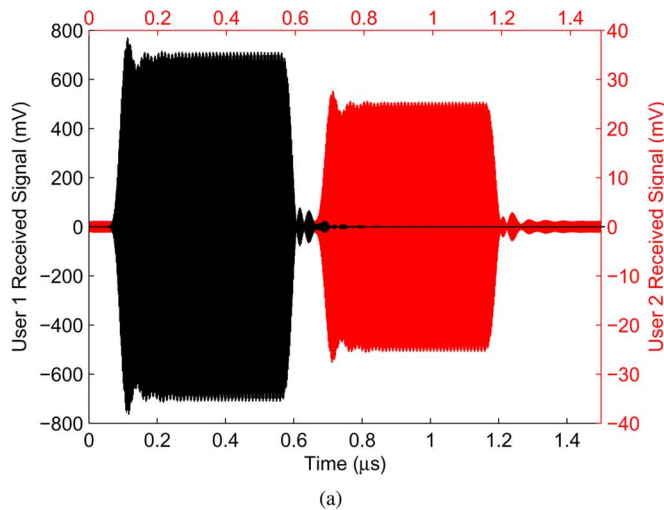


Fig. 8. Filtered frequency-hopping pulses. 900-MHz seventh-order 4% Chebyshev filter. User 1 at 10 dBm, User 2 at -20 dBm, 900-MHz frequency, 100-ns guard band. (a) Individual pulses; larger voltage and time scale; User 1's pulse overlaps User 2's pulse near $t = 0.7 \mu\text{s}$. (b) Pulse envelopes; voltage and time scale focused on the overlap region; RF carriers removed for visual clarity; User 1's residual tail is clearly visible within User 2's timeslot.

is the center frequency of the filter, the condition for minimum pulse overlap.

The trend in Fig. 9 is intuitive: a larger guard-band reduces the signal power that spills over from User 1's transmission into User 2's time slot. One result from the plot is surprising, however: even for guard bands that last a hundred RF cycles, the SIR, considering only the transient response of the bandpass filter, may be only 5–10 dB. This data shows that an additional degree of caution is necessary when designing a bandpass frequency-hopping scheme such that the transients produced by the basestation filter do not result in intersymbol interference (ISI) between user transmissions.

If transient filter properties should produce intolerable ISI, several techniques can be used to mitigate the problem. For a fixed filter architecture, an increase in guard banding between pulses would reduce pulse overlap, thereby directly reducing ISI. For a fixed data rate, a decrease in filter order would also reduce pulse overlap by shortening each pulse's residual tail. If neither the filter architecture nor the data rate can be changed,

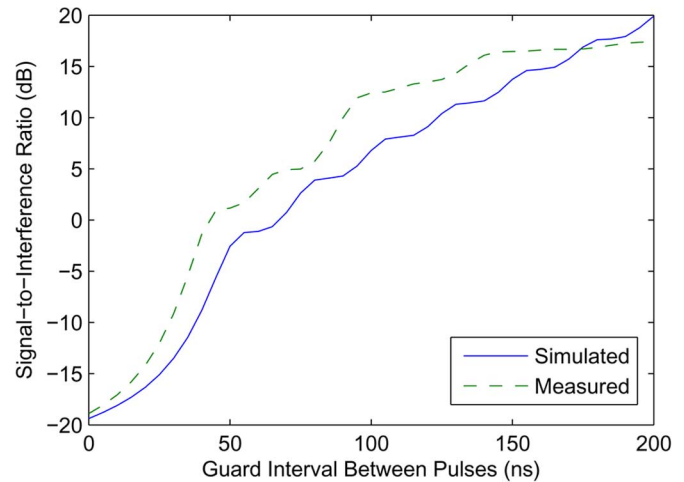


Fig. 9. Signal-to-interference ratio as a function of guard interval length. User 1 at 10 dBm, User 2 at -20 dBm, 900-MHz frequency; signal power received from User 1 after the guard band is integrated over the duration of User 2's pulse and treated as interference energy.

the ambiguity of overlapping pulses may yet be avoided by coding hopping sequences that do not repeat frequencies between users in adjacent time-slots. In any case, it is the responsibility of the system designer to evaluate these options so that the basestation filter—a component whose behavior is not widely known to produce co-site interference—does not degrade the communication system's performance.

VII. CONCLUSIONS

The analysis of RF systems has been performed primarily in the frequency domain. Since steady-state is assumed, the transient behavior of RF networks is generally ignored. As systems with narrower bandwidths and sharper band-limiting characteristics are implemented, however, it becomes necessary for resonant structures to store more field energy to produce more rigid frequency-domain characteristics, and the time required to charge and discharge the structures is extended. Measurements show that narrowband transients in cellular-band communications filters can last for hundreds of RF cycles, a time period that is significantly longer than conventional time-bandwidth rules of thumb. The transient behavior of narrowband components can no longer be ignored.

The cause of long-tail transients in bandpass filters is tied to the physical structure of its resonant cascade. Interference patterns can be produced at the output of a filter by switching the frequency of the signal applied to its input faster than the settling time of its resonators. Measurements confirm that two-tone interference is present at the output of a narrowband filter when the frequency of a single input tone is stepped closer to the center of the filter's passband.

The systems that are most likely to be affected by longer-than-expected transient behavior are those that use time-division schemes with pulse lengths that approach the duration of the transients, such as fast-frequency-hopping. The long-tail response produced by filtering stronger signals has the potential to overlap the reception of weaker signals, leading to a reduced signal-to-interference ratio.

REFERENCES

- [1] J. R. Wilkerson, K. G. Gard, A. G. Schuchinsky, and M. B. Steer, "Electro-thermal theory of intermodulation distortion in lossy microwave components," *IEEE Trans. Microw. Theory Tech.*, vol. 56, no. 12, Dec. 2008.
- [2] J. R. Carson and T. C. Fry, "Variable-frequency electric circuit theory with application to the theory of frequency modulation," *Bell Syst. Tech. J.*, vol. 16, pp. 513–540, Oct. 1937.
- [3] D. G. Tucker, "Transient response of filters," *Wireless Eng.*, vol. 23, pp. 36–42, Feb. 1946.
- [4] D. G. Tucker, "Transient response of filters," *Wireless Eng.*, vol. 23, pp. 84–90, Mar. 1946.
- [5] C. C. Eaglesfield, "Transient response of filters," *Wireless Eng.*, vol. 23, pp. 67–74, Mar. 1946.
- [6] C. C. Eaglesfield, "Transient response of filters," *Wireless Eng.*, vol. 23, pp. 306–307, Nov. 1946.
- [7] W. L. Hatton, "Simplified FM transient response," Massachusetts Inst. Technol., Cambridge, MA, Tech. Rep. 196, Apr. 1951.
- [8] R. E. McCoy, "FM transient response of band-pass circuits," *Proc. IRE*, vol. 42, no. 3, pp. 574–579, Mar. 1954.
- [9] H. Salinger, "Transients in frequency modulation," *Proc. IRE*, vol. 30, no. 8, pp. 378–383, Aug. 1942.
- [10] D. D. Weiner and B. J. Leon, "The quasi-stationary response of linear systems to modulated waveforms," *Proc. IEEE*, vol. 52, no. 6, pp. 564–575, Jun. 1965.
- [11] H. Hartley, "Transient response of narrow-band networks to narrow-band signals with applications to frequency-shift keying," *IEEE Trans. Commun. Technol.*, vol. 14, no. 4, pp. 470–477, Aug. 1966.
- [12] V. C. Chohan and J. K. Fidler, "Generalised transient response of band-pass transfer functions to FSK and PSK-type signals," *Electron. Lett.*, vol. 9, no. 14, pp. 320–321, Jul. 1973.
- [13] D. Kajfez and P. Guillon, *Dielectric Resonators*. Atlanta, GA: Noble, 1998.
- [14] H. J. Blinichkoff and A. I. Zverev, *Filtering in the Time and Frequency Domains*. Raleigh, NC: SciTech, 2001.



Gregory J. Mazzaro (S'04) was born in Bronxville, NY. He received the B.S. degree in electrical engineering from Boston University, Boston, MA, in 2004, the M.S. degree in electrical engineering from The State University of New York, Binghamton, in 2006, and is currently working toward the Ph.D. degree at North Carolina State University, Raleigh.

In 2006, he interned as a Research Scientist with the Air Force Research Laboratory, Rome, NY. In 2007, he was an Electronics Engineer for the Army Research Laboratory, Adelphi, MD. He is currently a

Graduate Research Assistant with the Electronics Research Laboratory, Department of Electrical and Computer Engineering, North Carolina State University. His research interests are RF circuits, wave propagation and antennas, and remote detection and characterization of electronic devices.



Michael B. Steer (S'76–M'82–SM'90–F'99) received the B.E. and Ph.D. degrees in electrical engineering from the University of Queensland, Brisbane, Australia, in 1976 and 1983, respectively.

He is currently the Lampe Professor of Electrical and Computer Engineering with North Carolina State University, Raleigh. In 1999 and 2000, he was Professor and Director of the Institute of Microwaves and Photonics, The University of Leeds, where he held the Chair in Microwave and Millimeter-Wave Electronics. He has authored 400 publications on topics related to nonlinear RF effects, circuit-field simulation, RF behavioral modeling, microwave and millimeter-wave systems, high-speed digital design, and RF/microwave design methodology. He is an expert on circuit-field interactions. He authored *Microwave and RF Design: A Systems Approach* (SciTech, 2008) and coauthored *Foundations of Interconnect and Microstrip Design* (Wiley, 2000) and *Multifunctional Adaptive Microwave Circuits and Systems* (SciTech, 2009).

Prof. Steer was the secretary of the IEEE Microwave Theory and Techniques Society (MTT-S) in 1997. From 1997 to 2000 and 2003 to 2006, he was a member of the IEEE MTT-S Administrative Committee (AdCom). He was Editor-in-Chief of the IEEE TRANSACTIONS ON MICROWAVE THEORY AND TECHNIQUES from 2003 to 2006. He was a 1987 Presidential Young Investigator (USA). He was the recipient of the Bronze Medallion presented by the U.S. Army Research for "Outstanding Scientific Accomplishment" in 1994 and 1996. He was also the recipient of the Alcoa Foundation Distinguished Research Award presented by North Carolina State University in 2003.



Kevin G. Gard (S'92–M'95) received the B.S. and M.S. degrees in electrical engineering from North Carolina State University, Raleigh, in 1994 and 1995, respectively, and the Ph.D. degree in electrical engineering from the University of California at San Diego, La Jolla, in 2003.

He is currently the William J. Pratt Assistant Professor with the Electrical and Computer Engineering Department, North Carolina State University. From 1996 to 2003, he was with Qualcomm Inc., San Diego, CA, where he was a Staff Engineer and

Manager responsible for the design and development of RF integrated circuits (RFICs) for code-division multiple-access (CDMA) wireless products. He has designed SiGe BiCMOS, Si BiCMOS, and GaAs metal–semiconductor field-effect transistor (MESFET) integrated circuits for cellular and personal communication systems (PCSs) CDMA, WCDMA, and AMPS transmitter applications. His research interests are in the areas of integrated circuit design for wireless applications and analysis of nonlinear microwave circuits with digitally modulated signals. He has authored or coauthored over 60 papers related to RF/analog integrated circuit design and analysis of nonlinear circuits.

Dr. Gard is a member of Eta Kappa Nu and Tau Beta Pi. He is a member of the IEEE Microwave Theory and Techniques (IEEE MTT-S) Society and the IEEE Solid-State Circuits Society. In 2007, he was secretary of the IEEE MTT-S Administrative Committee (AdCom).



Aaron L. Walker (S'97–M'05) is a founder and Chief Technology Officer with Vadum Inc., Raleigh, NC. His research focuses on nonlinear metrology for remote characterization of RF and microwave systems, behavioral RF system modeling, and development of custom simulation environments. This includes the development of novel microwave measurement techniques and measurement-based behavioral models for describing the generation of complex nonlinear operation in microwave circuits. He has also been a Digital ASIC Designer in the

telecommunication industry and has been involved in startup efforts in robotics and medical instrumentation.